

Co-Designed High-Efficiency GaN Filter Power Amplifier

José Antonio Estrada^{#1}, Pedro de Paco[§], Seth Johannes[#], Dimitra Psychogiou[#], Zoya Popović[#]

[#]Department of Electrical Engineering, University of Colorado, USA

[§]Department of Telecommunications, Universitat Autònoma de Barcelona (UAB), Spain

¹Jose.Estrada@colorado.edu

Abstract—In this paper, we demonstrate a high-efficiency 4.7 GHz 4-W power amplifier with input and output matching networks designed as complex-impedance port filters, within a sub-6 GHz 5G band. The port impedances are determined by the load- and source-pull of a GaN HEMT for an efficiency-power tradeoff. The measured performance shows PAE=55% over a 9% fractional bandwidth, with 10 dB rejection at 4.5 and 5 GHz. Comparison with a cascaded PA-filter circuit shows 25% lower loss with a simultaneous 20% reduction in footprint.

Keywords— ceramic, coaxial resonators, GaN, power amplifiers, RF filters, 5G.

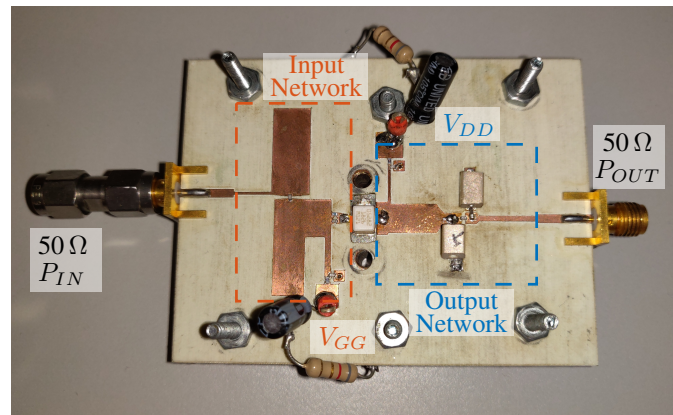
I. INTRODUCTION

Power amplifiers (PAs) in RF front-ends consume most of the power [1], and there is an ever-growing need to improve their efficiency as the signals in sub-6 GHz 5G bands become more challenging. In high-efficiency PAs, the transistors are driven into saturation, resulting in linearity degradation [2], [3]. Nonlinearity is exhibited as both in-band and out-of-band distortion. Both of these can be somewhat addressed with analog or digital predistortion (DPD) [4] but in many cases they require additional filtering to satisfy spectral masks. Out-of-band nonlinearities further from the signal up to harmonic frequencies are addressed by filtering. As more capacity is required in wireless communication, features like carrier aggregation make the problem of nonlinearities worse and filtering becomes more important.

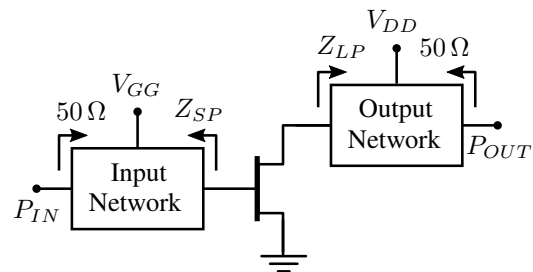
Filters are often cascaded at the input and output of a PA, increasing overall losses and size. Different applications favor either reduced loss (e.g. in higher power base-station transmitters) or reduced size (e.g. in portable devices). Integration of the lossy matching network and lossy filter can improve overall efficiency and reduce overall size. In [5] and [6] second and third order filter implementations integrated with a PA are presented at 3 GHz with 3 and 1.7 % bandwidth, respectively. In [7], [8] an active coupling matrix approach is shown, which follows from the analysis in [5] and [6], for linear amplifier design with a simple small signal model and implemented at 10 GHz with 5 % bandwidth. Here, we expand this concept by generalizing filter design for complex input and output impedances with n -th order filters, with a goal of reducing the overall size and loss of the RF front-end.

To synthesize the PA matching network with a specific filter response, the first challenge is to establish a filter design method with a complex load determined by the device nonlinear model, rather than the real load termination that is used in standard filter design methods [9]. In this work we present general equations for a simple modification of

the standard coupled-resonator filter synthesis approach to be valid for complex port impedances. We then validate this theory with a proof-of-concept 2nd order filter and integrated filter-PA (FPA) shown in Fig. 1.



(a)



(b)

Fig. 1. (a) Photo of the filter power amplifier (FPA) designed for operation at a center frequency of 4.7 GHz with a 9% bandwidth. (b) Block diagram of the FPA, where the input network is the co-designed input filter, matching network, stability network, bias line and harmonic termination. The output network is the co-designed output filter, matching network, bias line and harmonic termination, as shown in more detail within the dashed rectangle in Fig. 2b.

II. COMPLEX IMPEDANCE FILTER DESIGN THEORY

A traditional approach with filters cascaded with a PA is shown in Fig. 2a. Our approach from Fig. 1 with more details showing all relevant parts is presented in Fig. 2b. The bias lines, stability network, input and output harmonic terminations and matching networks are shown, highlighting the miniaturization advantage. Since transistors need to be matched to complex impedances for optimal operation, we next discuss our approach to filter design with complex ports. An n^{th} order filter where the source and load only couple to one resonator (1 and n in this case, respectively) is displayed

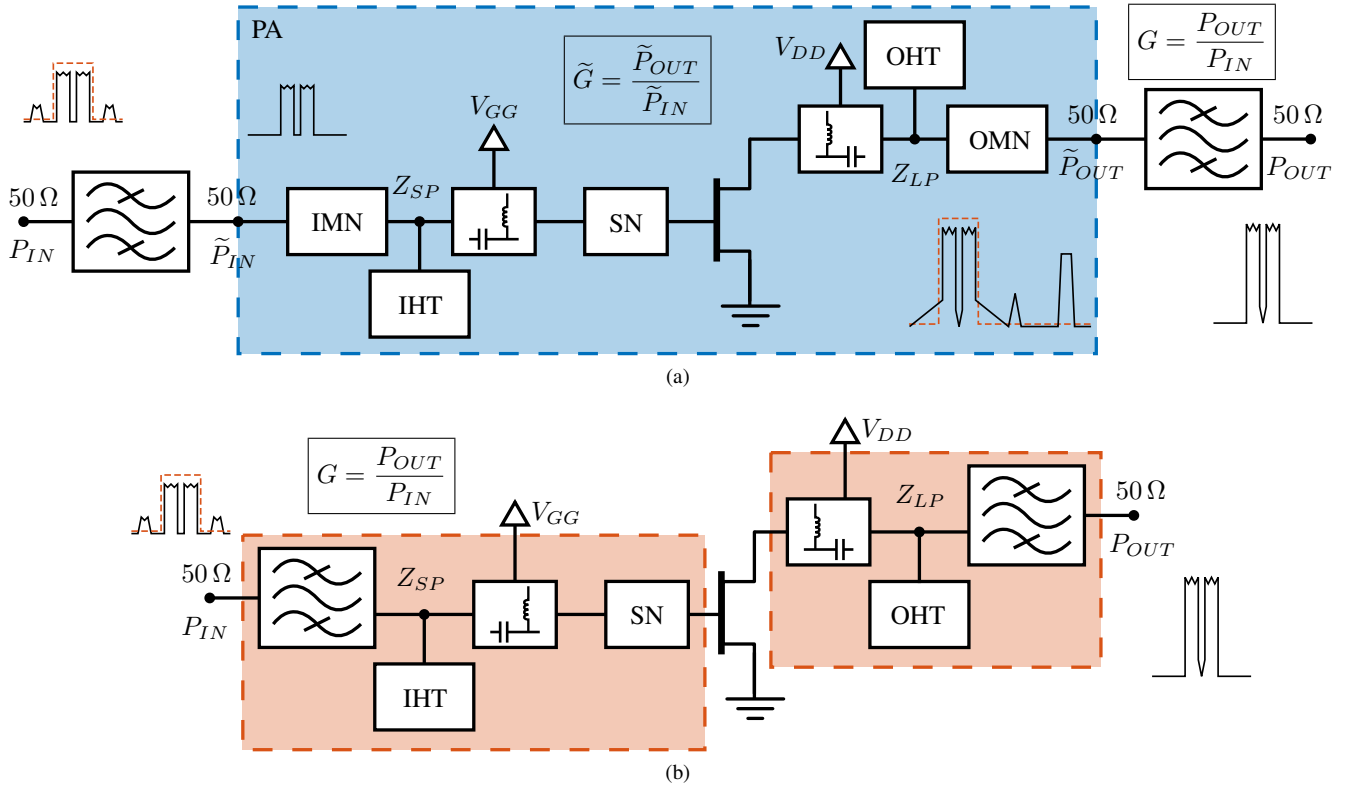


Fig. 2. (a) Block diagram of a power amplifier cascaded with filters at input and output, where the shaded area shows the PA alone. (b) Block diagram of the integrated filter with PA (FPA), where the input and output filters are the co-designed filter and matching circuits. The shaded input and output networks correspond with the ones shown in Fig. 1b.

in Fig. 3. This filter can be designed using the coupling matrix filter synthesis techniques as shown in [9], [10], where it is shown clearly how to obtain the elements in Fig. 3 from the coupling matrix. The frequency response of this filter is designed in normalized space (1Ω reference impedance and $\Omega = 1$ normalized angular frequency), where it does not depend on the source and load impedances.

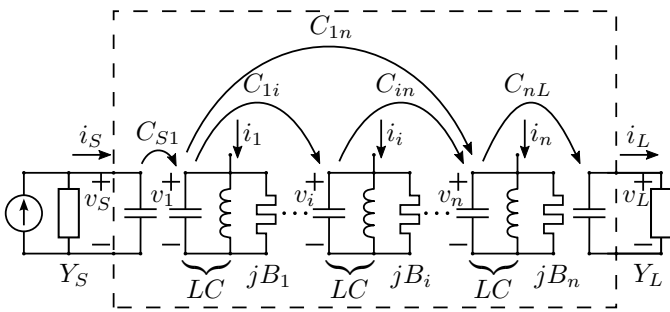


Fig. 3. Generic n^{th} order filter where the source and load couple only to one resonator.

Allowing a variation Δm_1 and Δm_n in the m_{11} and m_{nn} terms of a standard coupling matrix [9], respectively, the input and output impedances looking into the filter can be found as

$$z_{in} = \left[\frac{h_L(s, [m_0]) + s + jm_{11}}{m_{S1}^2} \right] + j \frac{\Delta m_1}{m_{S1}^2} \quad (1)$$

$$z_{out} = \left[\frac{h_S(s, [m_0]) + s + jm_{nn}}{m_{nL}^2} \right] + j \frac{\Delta m_n}{m_{nL}^2} \quad (2)$$

where s is normalized complex frequency, h_L and h_S are the equivalent admittances seen by the last/first resonators of the filter, which depend on all elements of the original normalized coupling matrix $[m_0]$ (without complex loading). Equations (1) and (2) hold given that the source and load impedances are

$$z_L = 1 - j \frac{\Delta m_n}{m_{nL}^2} = 1 + jx_L \quad (3)$$

$$z_S = 1 - j \frac{\Delta m_1}{m_{S1}^2} = 1 + jx_S \quad (4)$$

which leads to conjugate matching on both ports.

The terms in brackets in (1) and (2) do not explicitly depend on the resonator variations Δm_1 and Δm_n and are the frequency responses of a filter designed to work with resistive terminations. In band, these terms are very close or equal to one, indicating a good match. It can also be proven, but is beyond the scope of this paper, that the frequency response of the reflection coefficient of a filter terminated in the complex impedances (3) and (4) is exactly that of the resistively terminated filter ($\Delta m_1 = \Delta m_n = 0$).

The reactive part of the input and output port impedances can then be controlled by detuning the input (“1”) or output (“n”) resonators, respectively, while maintaining the same

filter response. The real part of the port impedance remains normalized and the necessary modification of the resonators can be found as

$$\Delta m_1 = -x_S m_{S1}^2 = -\frac{X_S}{R_S} m_{S1}^2 \quad (5)$$

$$\Delta m_n = -x_L m_{nL}^2 = -\frac{X_L}{R_L} m_{nL}^2 \quad (6)$$

where X_S and X_L are the reactive parts of the source and load impedances, respectively, while R_S and R_L are the real parts and are also the input and output port's normalizing impedances, respectively.

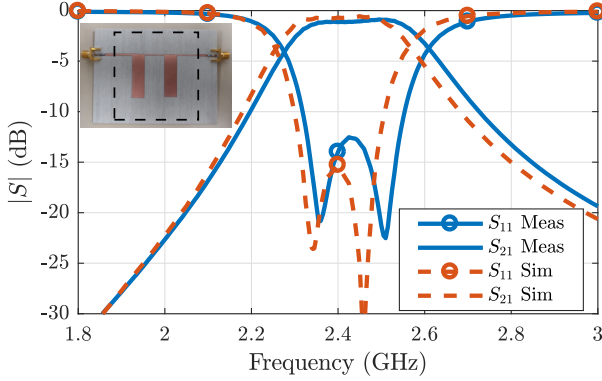


Fig. 4. Simulation and measurement results for the second order Chebyshev microstrip filter. The dashed rectangle in the photo frames the filter, $50\ \Omega$ sections are added to transition to the connectors, and in the measurements these are deembedded using TRL calibration.

III. FILTER IMPLEMENTATION

To verify the theory, a simple microstrip filter prototype using quarter-wave inverters and half-wave resonators was designed for $Z_S = (35 - j10)\ \Omega$ and $Z_L = (60 + j15)\ \Omega$. The filter has a second-order Chebyshev response with $R_L = 15\ \text{dB}$ and after modifying it for the complex impedance loading it has the following coupling matrix

$$[m] = \begin{bmatrix} 0 & 1.0369 & 0 & 0 \\ 1.0369 & 0.3072 & 1.2868 & 0 \\ 0 & 1.2868 & -0.2688 & 1.0369 \\ 0 & 0 & 1.0369 & 0 \end{bmatrix} \quad (7)$$

and is centered at $f_0 = 2.4\ \text{GHz}$ with 8% fractional bandwidth. This filter was designed and simulated using National Instrument's AWR for circuit and full-wave electromagnetic simulations. The filter was characterized and the frequency response can be seen in Fig. 4, where the port impedances are the complex values previously specified. Fig. 5 shows the reflection coefficients looking into the filter ports when the filter is terminated in the designed complex impedances. It can be seen that the impedances looking into the filter are conjugately matched to Z_S and Z_L in the passband (loop).

IV. FPA DEMONSTRATION

A filter integrated with a power amplifier (FPA) was designed to work in the sub-6 GHz range (FR1) of the 5G technical specification [11] utilizing filters as the matching

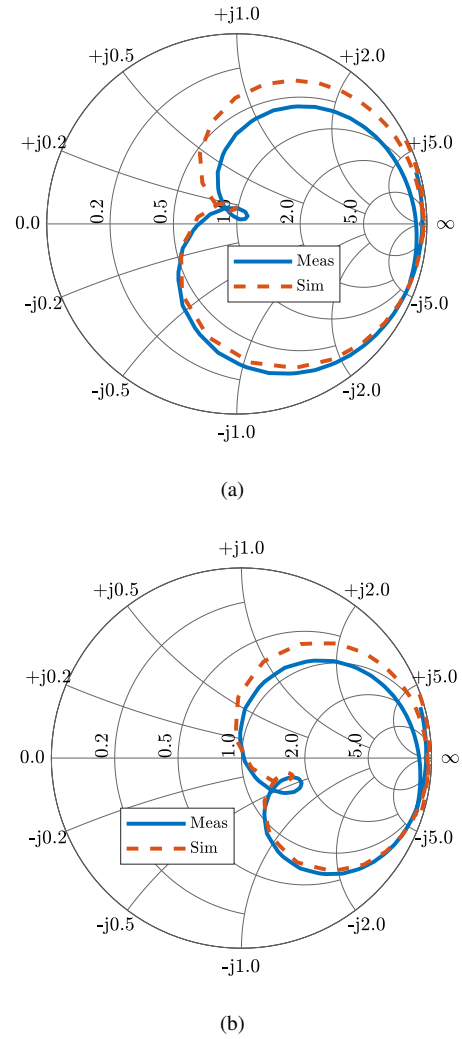


Fig. 5. Simulated and measured (a) S_{11} and (b) S_{22} for the filter.

networks and can be seen in Fig. 1. Due to the low Q -factor of microstrip resonators, and large impact of the output matching network loss on PA efficiency [12], we use ceramic coaxial resonators ($Q = 700$) in the output matching filter.

The PA is designed around Qorvo's T2G6000528-Q3 GaN transistor and is simulated using AWR's harmonic balance for the non-linear simulations with a Modelithics non-linear model for the transistor. The impedance matching filters (IMF) at the input and output are co-designed using Ansys HFSS full-wave EM simulations for modeling the resonators and NI-AWR for the rest of the circuit. These IMFs are designed to have a second order Chebyshev response with $R_L = 15\ \text{dB}$. Both IMFs have a center frequency of 4.7 GHz and 9% fractional bandwidth. The impedances of the filters and harmonic terminations are found using load-pull.

Small-signal measurements (Fig. 6) show that the FPA exhibits a filter response in both gain and input reflection coefficient (Γ_{IN}). Fig. 7 presents the large-signal performance of the FPA at the peak PAE power output (P_{OUT}). The measured PAE for the FPA at the center and the edges of the band is shown in Fig. 8. The PAE reaches 55% at 4.7 GHz

with a saturated gain of 13.7 dB. Comparison with simulations for a cascaded PA-filter circuit is shown in Fig. 9, showing 25% lower loss with 20% reduction in footprint for the co-designed FPA.

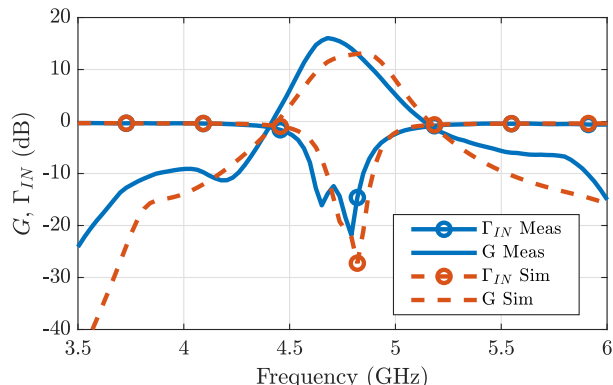


Fig. 6. Measured and simulated small-signal gain and input match of the FPA from Fig. 1. The gain is within 3 dB of the simulated value.

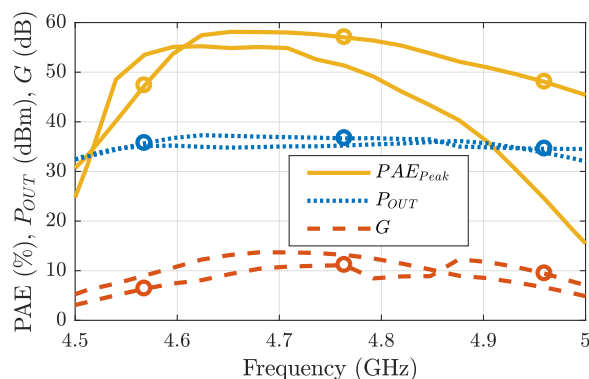


Fig. 7. FPA large-signal simulations and measurements as a function of frequency, where the traces with symbols represent simulations.

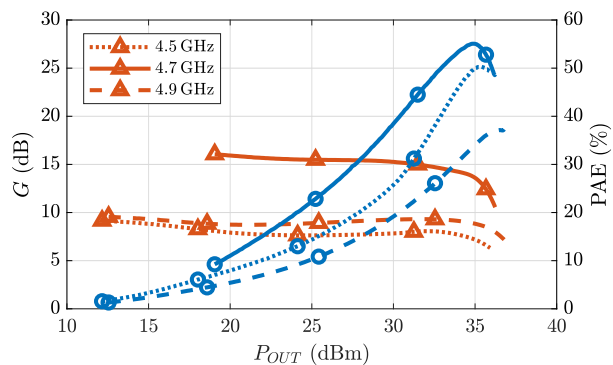


Fig. 8. Measured PAE as a function of P_{OUT} for the FPA at the center and edges of the band.

V. CONCLUSION

In summary, we demonstrate a high-efficiency 4.7 GHz 4-W filter power amplifier (FPA) with PAE=55% over a 9% bandwidth, with 10 dB rejection at 4.5 and 5 GHz. The input and output matching networks are designed as filters with a complex impedance port, given by the load- and source-pull impedances of the GaN HEMT for an efficiency-power trade-off. The biasing, 2nd and 3rd harmonic terminations are also

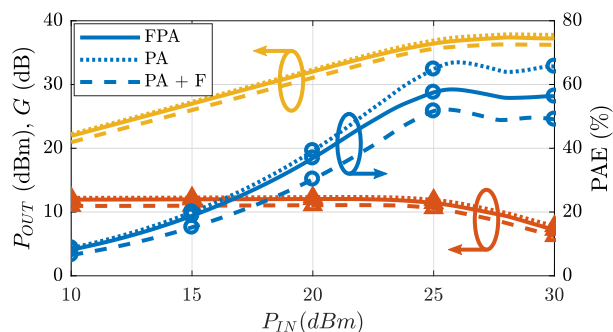


Fig. 9. Simulation comparison between the designed FPA, a PA where the output matching network is made with a more traditional stub matching and that same PA cascaded with a filter designed in the same way as the one in the FPA but using $50\ \Omega$ ports on both sides.

co-designed to achieve a compact and low-loss circuit. The fundamental impedance match at the output is implemented with surface-mount high- Q ceramic coaxial resonators with a 2nd-order Chebyshev filter response. Compared to a cascaded PA and filter, we show 25% lower loss and 20% reduction in footprint.

ACKNOWLEDGMENT

This work was funded in part by a NSF SpecEES grant ECCS-1731956.

REFERENCES

- [1] B. Manz, "Rf power amplifier efficiency: Big challenges for designers," 2015 (accessed November, 2019), original document from Mouser Electronics. [Online]. Available: https://www.mouser.com/publicrelations_techarticle_rf_power_amp_efficiency_2015final
- [2] J. Wood, *Behavioral Modeling and Linearization of RF Power Amplifiers*, ser. Artech House Microwave Library. Artech House, 2014.
- [3] S. Cripps, *RF Power Amplifiers for Wireless Communications*, ser. Artech House microwave library. Artech House, 2006.
- [4] Lei Ding *et al.*, "A robust digital baseband predistorter constructed using memory polynomials," *IEEE Transactions on Communications*, vol. 52, no. 1, pp. 159–165, Jan 2004.
- [5] K. Chen, J. Lee, W. J. Chappell, and D. Peroulis, "Co-design of highly efficient power amplifier and high- q output bandpass filter," *IEEE Transactions on Microwave Theory and Techniques*, vol. 61, no. 11, pp. 3940–3950, Nov 2013.
- [6] K. Chen, T. Lee, and D. Peroulis, "Co-design of multi-band high-efficiency power amplifier and three-pole high- q tunable filter," *IEEE Microwave and Wireless Components Letters*, vol. 23, no. 12, pp. 647–649, Dec 2013.
- [7] Y. Gao, J. Powell, X. Shang, and M. J. Lancaster, "Coupling matrix-based design of waveguide filter amplifiers," *IEEE Transactions on Microwave Theory and Techniques*, vol. 66, no. 12, pp. 5300–5309, Dec 2018.
- [8] Y. Gao *et al.*, "Integrated waveguide filter amplifier using the coupling matrix technique," *IEEE Microwave and Wireless Components Letters*, vol. 29, no. 4, pp. 267–269, April 2019.
- [9] R. Cameron, C. Kudsia, and R. Mansour, *Microwave Filters for Communication Systems*. Wiley, 2015.
- [10] J. Hong and M. Lancaster, *Microstrip Filters for RF / Microwave Applications*, ser. Wiley Series in Microwave and Optical Engineering. Wiley, 2004.
- [11] *Technical Specification Group Radio Access Network; NR; Base Station (BS) radio transmission and reception (Release 15)*, 3rd Generation Partnership Project Std., Sep. 2018.
- [12] P. J. Bell, Z. Popovic, and C. W. Dyck, "Mems-switched class-a-to-e reconfigurable power amplifier," in *2006 IEEE Radio and Wireless Symposium*, Oct 2006, pp. 243–246.